Quantitative Interpretation of Light Beam Induced Current Contrast Profiles: Evaluating the influence of a near grain boundary

G. Micard[1], S. Seren[1], G. Hahn[1]
[1] University of Konstanz, Department of Physics, Jacob-Burckhardt-Str. 29, 78464 Konstanz, Germany

ABSTRACT: The quantitative interpretation of a Light Beam Induced Current (LBIC) contrast profile (LBIC signal normalized to the signal infinitely far from the grain boundary) of a Grain Boundary (GB) allows the estimation of the effective diffusion length in the neighboring grains (L_{eff}) as well as the recombination strength of the GB characterized by its equivalent Surface Recombination Velocity (SRV) v_s. Among the various sources of asymmetry of GB contrast profile, the presence of a nearby GB (less than one L_{eff} from the studied GB) is one of the most present in mc-Si wafer solar cells. We show here that fitting these asymmetric profiles using a different diffusion length on each side of the GB induces, additionally to a erroneous fit shape, a large error in the grain diffusion length estimation. In order to be able to fit this situation, we present here a dedicated model that takes in account the influence of nearby grain boundary on one side providing that the next grain boundary on the other side is located at more than 1.5 L_{eff}. In a future extension, this technique will present the unique feature of being able to evaluate the diffusion length of elongated narrow grains, like in silicon ribbon materials, that cannot be usually accessed because of the predominant influence of the GB on their plateau level.
Keywords: Recombination, Grain boundaries, Modeling

1 INTRODUCTION

Donolato derived expressions for EBIC and LBIC contrast profiles [1] (profile normalized to the signal infinitely far from the GB, the so-called plateau level). A fundamental limitation of Donolato's model lies in the symmetry of the case he studied: 1 GB with same diffusion length on both sides (referred as 'one L_{eff} ' model). Therefore the profiles calculated are symmetrical around the studied GB. In the most likely case where the profile is not symmetrical, there could be 2 main causes for this asymmetry: different diffusion length on either side of the GB or different size of the neighboring grains which induces a different influence of the next GB on each side (different plateau levels).

On the first cause of asymmetry we developed in our former study [2] a model to take this effect into account that will be referred here as the 'two L_{eff} 'model.

On the second cause of asymmetry, Von Roos and Luke [3] derived expressions for the profile point source solution when there is a second GB (with SRV S_2) at a distance w from the first (with SRV S_1) assuming the same diffusion length everywhere. They show that, when w becomes of the order of the diffusion length or below, the profiles are strongly distorted. We observed that, for w up to 2 L_{eff}, there is an apparent lowering of the plateau level on the second GB side. This phenomenon can lead to an erroneous fit if the profile is normalized referring to this plateau level.

Providing that the next GB on the other side is located at more than 2 L_{eff} from the studied GB, the profile can be normalized to the plateau of this side and can be investigated by an adaptation of the work of Von Roos and Luke for the LBIC profile.

We performed this extension making use of the formalism of Donolato, assuming a Gaussian profile for the LASER beam, and derived an analytical expression for a LBIC profile that is referred here as the 'two SRV' model.

After presenting the application of our fitting procedure to some typical examples we will present a comparison between different models and discuss about their limitations. Finally we'll discuss the possible improvements in order to increase reliability and robustness of this model.

2 THEORY OF THE 'TWO SRV MODEL'

2.1 Diffusion problem

The theoretical contrast profile expression is obtained assuming that the collected charges in the emitter are the minority carriers driven only by diffusion. Under such conditions, the minority carrier continuity equation alone is suitable to describe the problem.

$$D_p \Delta p(r) - \frac{1}{\tau} p(r) = -g(r) \qquad (1)$$

Here D_p is the minority carrier diffusion constant, τ the minority carrier lifetime, g(r) the volume generation function and p(r) the minority carrier density at point r.

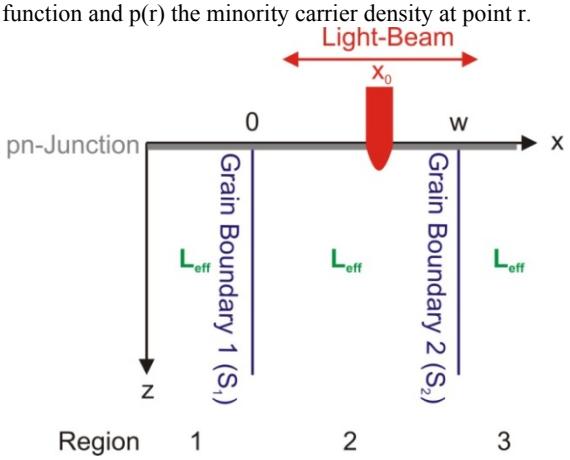

Figure 1: Schematic of the diffusion problem

Requirements and justifications of the model can be found in [2]

Therefore the problem can be schematically represented according to Fig. 1, in which the 2 GB (that are separated by a distance w) divide the volume in 3 regions and the junction is represented as an infinitely recombinative surface

$$p(r)|_{z=0} = 0 \qquad (2)$$

At the GB's , a first condition imposes the continuity of the carrier concentration

$$p(r)|_{x=0^+} = p(r)|_{x=0^-} \quad (3a)$$
$$p(r)|_{x=w^+} = p(r)|_{x=w^-} \quad (3b)$$

Where w is the distance between the 2 GB.

The second condition relates the total minority carrier flux at the GB's to the local carrier density introducing $S_{1,2}$, the surface recombination velocity at GB 1 and 2.

$$D_p \left.\frac{\partial p}{\partial x}\right|_{x=0^+} - D_p \left.\frac{\partial p}{\partial x}\right|_{x=0^-} = S_1 . p(r)|_{x=0} \quad (4a)$$
$$D_p \left.\frac{\partial p}{\partial x}\right|_{x=w^+} - D_p \left.\frac{\partial p}{\partial x}\right|_{x=w^-} = S_2 . p(r)|_{x=w} \quad (4a)$$

Then the measured current collected at the junction is found by integrating the normal gradient of p(r) (solution of (1) with boundary conditions (2,3,4)) at the surface plane z=0 times the elementary charge q

$$I = q . D_p \int_{-\infty}^{\infty} \left.\frac{\partial p}{\partial z}\right|_{z=0} dx\, dy \quad (5)$$

2.2 Carrier collection probability and volume generation function

Following the formalism of Donolato the collected current can be described more adequately by an equation structurally equivalent to the convolution product of the carrier collection probability (Q) for a point source (ps) located at (x_{ps}, z_{ps}) in the semiconductor times the function h which is the projection in the x,z plane of the volume generation function (g) induced by an electron/laser beam centered at x_0.

$$I(x_0) = q . \int_{-\infty}^{\infty} \int_0^{\infty} Q(x_{ps}, z_{ps}) \cdot h(x_{ps} - x_0, z_{ps}) dz_{ps}\, dx_{ps} \quad (6)$$

$$h(x,z) = \int_{-\infty}^{\infty} g(x,y,z) dy \quad (7)$$

Deriving the carrier collection probability, we have 3 cases to distinguish depending if the point source is region 1, 2 or 3. Considering that, wherever the point source is located, each region will have its contribution to the collected current, both SRV and Leff are introduced in the expressions of the collection probability. Then for Q_1 (the subscript 1 indicates that the point source is in region 1 (x_{ps}<0)) we obtain:

$$Q_1(x_{ps}, z_{ps}) = exp\left(-\frac{z_{ps}}{L_{eff}}\right) - \frac{2}{\pi} \cdot \int_0^{\infty} \frac{k}{\mu^2} \cdot \frac{\left[\frac{s_1 . e^{2\mu . w} . (2\mu + s_2) +}{s_2 . (2\mu . e^{\mu . w} - s_1)}\right] . e^{\mu . x_{ps}}}{e^{2\mu . w} . (2\mu + s_1)(2\mu + s_2) - s_1 . s_2} sin(k \cdot z_{ps}) dk \quad (8)$$

With

$$\mu = \sqrt{k^2 + \frac{1}{L_{eff}^2}} = \sqrt{k^2 + \frac{1}{D_p . \tau}} \quad (9)$$

and $s_{1,2}$ the reduced SRV for GB 1,2

$$s_{1,2} = \frac{S_{1,2}}{D_p} \quad (10)$$

A similar expression can be obtained for Q_3 exchanging the index 1 and 2 and taking w–x_{ps} instead of x_{ps}.

For Q_2 we obtain

$$Q_2(x_{ps}, z_{ps}) = exp\left(-\frac{z_{ps}}{L_{eff}}\right) - \frac{2}{\pi} \int_0^{\infty} \frac{k}{\mu^2} . \frac{\left[\frac{s_1 . ((2\mu + s_2) . e^{\mu . w} - s_2) . e^{\mu . (w - x_{ps})} +}{s_2 . ((2\mu + s_1) . e^{\mu . w} - s_1) . e^{\mu . x_{ps}}}\right]}{e^{2\mu . w} . (2\mu + s_1)(2\mu + s_2) - s_1 . s_2} . sin(k . z_{ps}) . dk \quad (11)$$

As shown in [2], for a Gaussian Laser beam, h has the following expression:

$$h(x,z) = C_1 \cdot exp\left(-\frac{x^2}{\sigma^2}\right) \cdot exp(-\alpha . z) \quad (12)$$

with

$$C_1 = A \cdot \alpha \cdot \eta \cdot (1 - R) \cdot \sqrt{\pi} \cdot \sigma \quad (13)$$

With A the laser beam intensity, α the absorption coefficient at the laser wavelength (72 mm^{-1} for silicon at 833 nm), η the quantum efficiency, R the reflection coefficient and σ the standard deviation of the beam

2.3 Plateau current and normalization

In order to obtain I, we have thus to integrate separately Q_1 for all x_{ps}<0 and Q_2 for all 0<x_{ps}<w and Q_3 for all x>w in (6).

Donolato showed that the first term in the expression of Q (8) will lead to an additive constant in the expression of the current corresponding physically to the plateau current or the current obtained very far or without a GB (I_0). We normalized the expression by I_0 that allows removing the constant C1 which depend of parameters difficult to estimate.

The final result is therefore (14) in which the result of Donolato [1] for 1 GB could be retrieved by setting s_2=0 (no second GB) or w→∞ (second GB infinitely far).

3 IMPLEMENTATION AND APPLICATION

3.1 Implementation

A graphical interface was developed under Matlab to estimate the parameters. We observed that the parameters extracted are so sensitive to small variations of the profile that a full optimization algorithm can easily lead to large errors in the parameters estimations while being highly time consuming. We therefore preferred to implement a simple trial and error method.

The "exp(x²)erfc(x)" term require a special evaluation procedure described in [2].

The improper integral in (14) is evaluated using the Gauss-Kronrod quadrature.

The plateau level determination is very critical in order to estimate accurately the diffusion lenght (particularly in the case of long diffusion lengths [4]). After trying to determine it by an average value of the most inner zone of the concerned grain, we realized that this method was not accurate enough for reaching accuracy below 1% on the plateau value. We introduced then a more suitable method based on the estimation of a scaling factor on an interval of confidence.

If we discard any offset current due to the LBIC instrument, the theory foresees that the simulated profile should differs from the measured profile only by a scaling factor if the plateau is not accurately set. This factor can therefore be estimated by proportionality interpolation between simulated and measured data.

The user can then determine where the plateau data are the most reliable regarding the plateau (or quasi plateau) shape and set this part as interval of confidence. The algorithm will compute the optimal scaling factor for this part and scale the whole profile by it. If the interval of confidence is correctly set, this method finely tunes the plateau value to optimal value according to each new parameters trial.

$$\frac{I(x_0)}{I_0} = 1 - \frac{1}{\pi}\left(\frac{1}{L_{eff}} + \alpha\right).\int_0^{\infty} \left[e^{\mu.x_0}.\begin{bmatrix} s_1.\left((2\mu + s_2) - s_2 e^{-\mu.w}\right).Erfc\left(\frac{\mu.\sigma}{2} + \frac{x_0}{\sigma}\right) + \\ e^{-\mu.w}.s_2.\left((2\mu + s_1).-s_1.e^{-\mu.w}\right).Erfc\left(\frac{\mu.\sigma}{2} - \frac{w-x_0}{\sigma}\right) \end{bmatrix} + \right. \left. e^{\mu.(w-x_0)}.\begin{bmatrix} s_2.\left((2\mu + s_1) - s_1.e^{-\mu.w}\right).Erfc\left(\frac{\mu.\sigma}{2} + \frac{w-x_0}{\sigma}\right) + \\ e^{-\mu.w}.s_1.\left((2\mu + s_2) - s_2.e^{-\mu.w}\right).Erfc\left(\frac{\mu.\sigma}{2} - \frac{x_0}{\sigma}\right) \end{bmatrix} \right] dk \quad (14)$$

$$\frac{k^2.e^{\left(\frac{\mu.\sigma}{2}\right)^2}}{(k^2+\alpha^2).\mu^2.\left((2\mu+s_1)(2\mu+s_2)-s_1.s_2.e^{-2\mu.w}\right)}.$$

3.2 Application

We have to remind that the assumptions used to establish this model do not allow us to study all the grain boundaries.

The suitable ones have to be selected according to the following criteria:

- The GB has to be relatively straight around the cutting point and relatively homogenous in its direction (assumption of invariance along the y axis).
- An absolute plateau level is an important condition for estimating L_{eff} and therefore we need at least 1 grain that is larger than 1.5 L_{eff} in the cutline direction.

3.3 Results

We measured a high resolution LBIC map (2 µm resolution) using a finely focused laser beam ($\sigma \approx 7\mu m$) of a solar cell fabricated using multicrystalline float zone silicon described in [5].

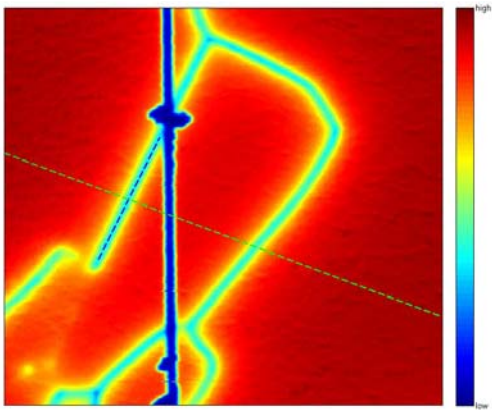

Figure 2: LBIC map of short circuit current @ 833 nm for a two GB situation

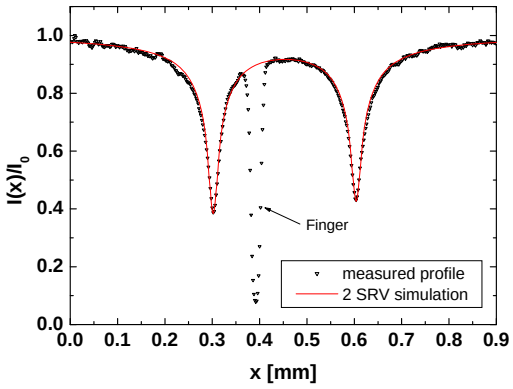

Figure 3: Normalized profile of the two GB situation at the cutline defined in figure 2

We can see on the LBIC map of Fig.2 the linescan of the grain boundary (dashed green line) performed perpendicularly to the GB direction (dashed blue line).

After normalization by the plateau level and evaluating the position of GB1 and GB2, the profile is fitted according to our model with L_{eff}= 1mm, S_1=3.2*10^5 cm/s and S_2 =1.8*10^5 cm/s assuming a diffusion coefficient D_p=28 cm^2/s (Fig. 3). We can observe that the finger involuntary present has no influence on the shape of profile, except of course at its own location.

The excellent fit of the overall profile indicate therefore that the diffusion length is the same in each region. Therefore, the lowering of the level in the central region is only due to the influence of both GB being distant of only ≈L_{eff}/3 and not to a different diffusion length.

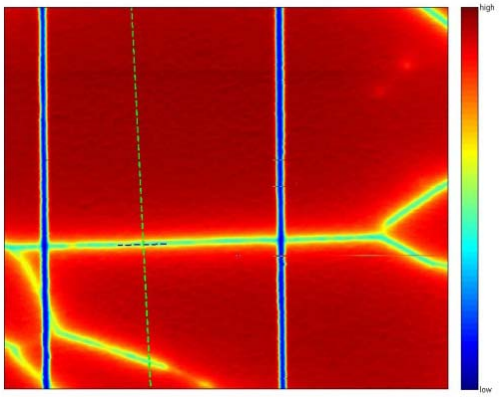

Figure 4 : LBIC map of short circuit current @ 833 nm for another two GB situation

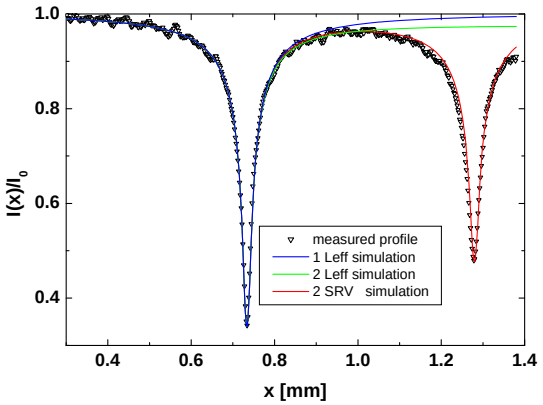

Figure 5 :comparison between 'One Leff' 'Two Leff' and 'Two SRV' model at the cutline defined in figure 4

On another two GB situation (Fig.4), we compared

the extracted parameters of the 'One Leff' 'Two Leff' and 'Two SRV' model assuming the most accurate fit of the left side of the profile.The parameter summary can be found in Table I.

The first grain boundary is accurately fitted by the 3 models considering the same value of the diffusion length L_{eff}=900 µm. This is in agreement with the very high SRV value of GB1 $S_1=2.8*10^6$ cm/s which prevent any carrier transfer from the left to the right side and makes the fitting of the left side independent of the one of the right side. The investigated models differ only on the treatment of the right side whereas they agree on the value of the left side.

We observed that while the '1 L_{eff} model' cannot take in account any lowering of the plateau level, the '2 L_{diff} model' can model the profile shape very accurately up to relatively close to the second GB. However the present lowering of the second plateau results in a diffusion length of 350 µm on the right side to be compared with the 900 µm on the other side. In the end, our '2 SRV model' provided an accurate fit on both sides (with $S_2=1.2*10^5$ cm/s) meaning that the diffusion length is likely to be the same everywhere. Therefore, even correctly fitting most of the intra grain region, the '2 L_{eff} model' leads to erroneous fitting parameters when the asymmetry is induced by a second GB.

Table I: summary of the 3 model comparison

One L_{eff}		Two L_{eff}		Two v_s	
L_1 [µm]	900	L_1[µm]	900	L_1 [µm]	900
v_{s1}[cm/s]	$2.8*10^6$	v_{s1}[cm/s]	$2.8*10^6$	v_{s1}[cm/s]	$2.8*10^6$
		L_2[µm]	350	v_{s2}[cm/s]	$1.2*10^5$

3 DISCUSSION ON THE LIMITATIONS

As already mentioned, in the case of very high diffusion lengths, the diffusion length determination is strongly dependent of the plateau value determination. In order to discard the influence of the laser reflection (present in the constant C1) we assumed it to be homogeneous over the whole profile. This assumption is not always suitable if we want to achieve a relative variation of less than 1% of C1 over the whole profile. Indeed, when the two neighboring grains have a different crystal orientation, it'll modify slightly their etching properties that turn to modify slightly their reflection properties. A future approach will be to normalize the profile by 1-R before the fitting procedure.

Other cause of asymmetry can be the non perpendicularity of the GB with the wafer surface. Simulations (Fig. 6) show that up to 20° of tilt angle, this influence could be neglected. We observe that this influence is more pronounced with increasing the wavelength of the laser. This phenomenon is due a higher penetration depth that induces perturbations on a larger distance scale. In the case of an asymmetric profile with the same plateau on both sides (no differing diffusion length) and no close GB, we could deduce that the grain boundary is tilted and is not relevantly fit with any model that does not take in account the tilt angle. Unfortunately a non perpendicular grain boundary is a non analytically solvable problem [6] and thus requires full numerical methods.

The influence on one side could be the result of a nearby GB and a different diffusion length. With our present model we could just say if the diffusion is larger (measurement higher than the simulated profile) or smaller (measurement lower than the simulated profile) than the diffusion on the other side, but it do not allows a quantitative estimation. A model combining these 2 aspects is therefore needed for further investigations.

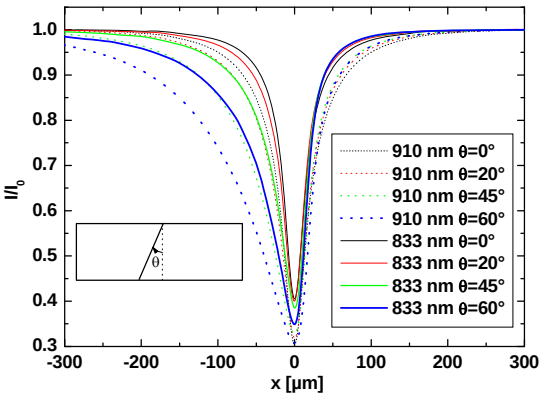

Figure 6 :Simulation of a grain boundary contrast profile when the GB is tilted by an angle θ with an infinite SRV, L_{eff}=100µm on a 250 µm thick structure for 910 and 833 nm Laser wavelenght.

4 FUTURE WORK

An inherent problem with the diffusion length estimation by this method occurs when the diffusion length is large because of the collection efficiency reaching one [4].

A long wavelength light, by penetrating deeper in the substrate, can bring more accurate determination of long diffusion length. We however face in this case that the dip becomes broader which shrinks the dimensions of the plateaus and increase the probability of not finding any plateau to scale accurately the profile.

We thought therefore of fitting a short wavelength profile, in which the plateau can be found easily but the accuracy on the parameter is relatively low, simultaneously with a longer wavelength profile, in which we can set as a first guess the previously fitted parameters and adjust manually the plateau value. The successful fitting of both profiles gives therefore more reliable parameters that the fitting of only one profile alone. This method could be extended to the 3 different wavelength of our LBIC system that could enhance its reliability and accuracy. Additionally, if some decrepency arise between the different wavelengths profile, the most likely explanation is that the wafer is not homogeneous in depth. The kind of decrepency encountered can bring some informations about the depth structure of the wafer around the cutline.

On string ribbon silicon materials, the crystals are elongated that makes them perfectly suitable for these models, and allow to study in detail their weak grain boundary and the diffusion in their narrow grain. However, the likely situation is to have a large grain and a succession of narrow grains. Even extended for different diffusion lengths, this model allow to study only the first narrow grain and get some hints on the second. To extend this model to an arbitrary number of GB we will have to use a full numerical approach. We intend to

develop a finite element method dedicated to this problem that is optimized regarding speed in order to get acceptable result accuracy for the same computation time as the evaluation of our present model theoretical expressions.

5 CONCLUSION

We generalized Donolato's theory for the case of the influence of a nearby GB. We compared the present model ('Two SRV model') with former models ('Two Leff' and 'One Leff' model) and demonstrate that additionally to the fact that the simulated shape cannot match the measured shape, the best fit leads to errouneous diffusion length estimation. However, several improvements are in development in order to make this method an even more reliable and robust tool for the investigation of grain boundaries in semiconductors.

6 REFERENCES

[1] C. Donolato, J. Appl. Phys. 54, 1314, 1983
[2] Micard G. et Al., Proc. EUPVSEC Valencia, 416, 2008
[3] K.L. Luke, O. von Roos, J. Appl. Phys. 55, 4275, 1984
[4] R. Corkish et al., J. Appl. Phys., 84 (10), 5473, 1998
[5] A. Zuschlag et al., Proc. EUPVSEC Valencia, 1915, 2008
[6] A. Mittiga et al., J. Appl. Phys.,63 (9), 4748, 1988